Received: 18 March 2019 | Revised: 19 August 2019 | Accepted: 5 September 2019

DOI: 10.1002/ese3.570

RESEARCH ARTICLE

Energy Science & Engineering Open Access

Experimental study on the enhanced oil recovery by in situ foam formulation

Hailong Chen[1,2] | **Zhaomin Li**[1] | **Fei Wang**[3] | **Aixin Li**[1] | **Silagi Wanambwa**[1] | **Teng Lu**[1]

[1]School of Petroleum Engineering, China University of Petroleum (East China), Qingdao, China

[2]Department of Petroleum and Geosystems Engineering, University of Texas at Austin, Austin, TX, USA

[3]Faculty of Electromechanical Engineering, Geo-Energy Research Institute, Qingdao University of Science and Technology, Qingdao, China

Correspondence
Zhaomin Li, School of Petroleum Engineering, China University of Petroleum (East China), Qingdao 266580, Shandong, China.
Email: lizhm@upc.edu.cn

Funding information
National Natural Science Foundation of China, Grant/Award Number: 51604292; Natural Science Foundation of Shandong Province, China, Grant/Award Number: ZR2016EEB29; National Science and Technology Major Project of China, Grant/Award Number: 2016ZX05012-002-004; Fundamental Research Funds for the Central Universities, Grant/Award Number: R1602013A; Fundamental Research Funds for the Central Universities, Grant/Award Number: 17CX02014A; Innovation Project Funds for the Central Universities, Grant/Award Number: YCX2017024

Abstract

In situ CO_2 foams (ISCF) are studied systematically by combining in situ CO_2 gas reactants (carbonate anhydrous, hydrochloric acid) and bio-based surfactant. Sandpack flooding experiments at 60°C along with PVT experiments were carried out to analyze the oil displacement mechanisms. The results showed that ISCF could increase oil recovery from heterogeneous multilayer formation of permeability ratio over 6, and displacement efficiency increased with the injection volume increased before the injection of 1 PV. The incremental oil recovery by ISCF was much greater than that of conventional foam or in situ CO_2 (ISC) without foam under the same injection conditions. The generated CO_2 foam could reduce the interfacial tension between displacement phase and displaced phase effectively which contributed to the great increase in capillary number. The CO_2 dissolution greatly reduced the viscosity of crude oil, and the highest viscosity reduction rate at 60°C could be as high as 98%. The Ca^{2+} concentration of produced liquids analysis revealed the ISCF could distribute intelligently the acid in heterogeneous formations.

KEYWORDS

in situ foam, intelligent acidification, interfacial tension reduction, viscosity reduction

1 | INTRODUCTION

CO_2 has unique physical properties like lower minimum miscible pressure (MMP) of CO_2 and crude oil compared with methane and nitrogen, making CO_2 an effective oil displacing agent.[1,2] With the increase in greenhouse gas emission reduction requirements, the application of CO_2 flooding technology is becoming more and more widespread. However, due to the large mobility ratio of CO_2 gas to crude oil, it is easy to cause gas channeling and gravity overburden in the

formation, resulting in low sweep coefficient during flooding, which greatly affects the displacement effect.[3-6] Therefore, effective control of CO_2 mobility is the key to improving its displacement.

In the 1960s, researchers first proposed the use of foam to control CO_2 gas flow.[7,8] Foam is a dispersion system formed by dispersing an insoluble or slightly soluble gas in a liquid. The gas surrounded by the liquid film forms a single bubble, and the foam is an aggregate of bubbles, wherein the gas is dispersive (discontinuous phase) and the liquid is a dispersion medium (continuous phase). This dispersion system can increase the apparent viscosity of the gas,[9-12] improve the ratio of CO_2 to crude oil flow, and has the characteristics of "selective blockage," so it can reduce the CO_2 mobility and increase the sweep coefficient,[13-17] thereby improving the displacement effect.[18-24] However, the injection of conventional foam requires special injection equipment and high injection pressure, which has great safety costs and operational limitations, and is not suitable for offshore oilfield platform operations. In addition, the transportation and storage of CO_2 gas sources will also greatly increase the economic operation cost.

Self-generated gas technology can effectively solve the storage and transportation problems of gas sources in offshore platform operation. Some early studies have proved its feasibility as a chemical flooding technique for enhanced oil recovery.[25-32] For example, Wang used urea and ammonium carbamate as reaction agents for the in situ CO_2 technology. They found that the in situ CO_2 technology was close to the complex combination flooding technology such as surfactant recovery and alkali flooding in terms of tertiary oil recovery.[25-27] In addition, the effects of injection method, agent concentration, and high divalent ion level on the reaction kinetics and recovery performance of the urea system were also investigated.[28,29] Zhu et al[30] used an acid-alternating base (AAB) system to generate CO_2 for blockage removal and enhanced oil recovery. Although in situ gas technology can improve oil displacement efficiency, it still faces the problem of mobility control of gas flooding technology.

Therefore, to overcome these problems and expand the foam application, in situ CO_2 foam method has been sought to replace the current conventional injection method. The potential benefits of this new method mainly including the following three aspects: (a) equipment and material aspect, ISCF system does not rely on the transportation pipeline and natural CO_2 source.[33,34] Besides traditional foam injection equipment requires high pressure capacity, ISCF can reduce the dependence on high pressure equipment, which contributes to the application and promotion in offshore oil fields. (b) Injection effect aspect, ISCF not only has better swept volume and cleaning efficiency than gas flooding, water alternating gas (WAG) flooding and carbonated water injection (CWI), but also unblock the contaminated formation to some extent. (c) Adaptation aspect, the formulation has exceptional salt, acid, and temperature tolerance for complicated reservoirs.

In this work, in situ CO_2 foam was firstly proposed by combining sodium carbonate anhydrous, hydrochloric acid, and bio-based surfactant. The production performance of in situ CO_2 foam system in heterogeneous formation and the effect of different injection volumes of chemical agents were initially investigated, and then, the interfacial tensions between surfactant solutions and crude oil were measured to analyze its effect on capillary number. Subsequently, PVT experiment was conducted to reveal the effect of CO_2 dissolution on crude oil viscosity and viscosity reduction rate at different gas-oil ratios and temperatures, and Ca^{2+} concentration of produced liquid was tested to explore the intelligent distribution of acid in heterogeneous multilayer formations. This technology not only takes advantage of the synergic combination of foam and in situ gas technology, but also extends the foam application in reservoirs.

2 | EXPERIMENTAL METHODS

2.1 | Experimental device

2.1.1 | Experimental device for sandpack flooding

Figure 1 presents the flooding device schematic diagram for ISCF experiment. The entire displacement system is divided into three parts, namely the injection part, the sandpack displacement part, and the gas-liquid collection part. The injection part mainly comprises intermediate containers and Teledyne ISCO pumps (model 100 DX) with the injection accuracy <0.25 μL/min, wherein the intermediate containers are used for holding liquids, including displacement water, gas-generating agent, gas-releasing agent, and ISCO pumps are used for controlling the injection velocity of liquids. The sandpack displacement part mainly consists of two horizontally placed sandpack holders for simulating water flooding, foaming agents flooding, and subsequent water flooding in reservoir conditions, in which four different pressure points are evenly distributed throughout the sandpack to observe real-time changes in pressure. The gas-liquid collecting part is mainly composed of back pressure valves and gas-liquid separators. The back pressure valves (BPR) are used to control the pressure of the whole experimental simulation system, and the gas-liquid separators are used for gas-liquid separation of the produced liquid.

Figure 2 shows the flooding device schematic diagram for conventional foam. Similar to the ISCF flooding device, the entire displacement system is also divided into three parts. The gas is supplied by a gas cylinder, and the flow rate of the

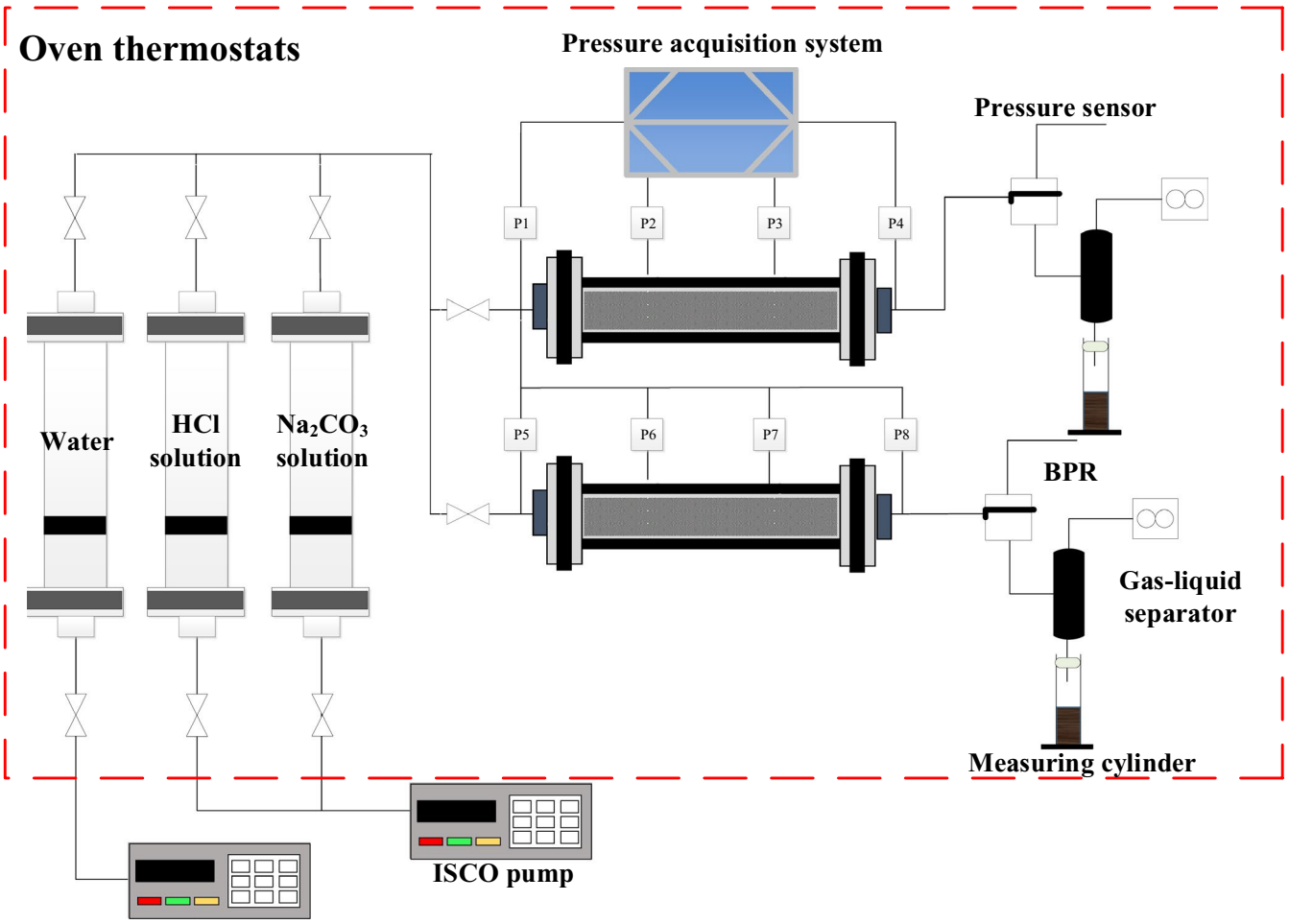

FIGURE 1 Schematic diagram of ISCF flooding experiment

gas is controlled by a mass flowmeter and a one-way valve. The water and surfactant solution are placed in intermediate vessels with the injection velocity controlled by ISCO pump. Foam generator is placed to pregenerate conventional foam before it is injected to sandpack flooding part. The sandpack displacement portion and the gas-liquid collection portion are identical to the ISCF displacement device.

2.1.2 | Experimental device for PVT test

Figure 3 presents the schematic diagram of experimental device for CO_2 dissolution PVT experiment. The device is divided into two parts, CO_2 dissolution part (zone 1) and viscosity measure part (zone 2). In zone 1, intermediate containers are prepared to hold the gas and heavy oil. The CO_2 and oil injection volume are controlled by mass flowmeter and ISCO pump. The injection rate is set below 10 mL/h to insure an accurate volume. A PVT cell with confining pressure controlled by a pressurization pump (with flow accuracy <0.25 μL/min and pressure accuracy <±0.5%) is fixed in a multifunctional displacement oven. The confining pressure is measured in MPa by a pressure gauge (measurement range of 30 MPa and an accuracy of 0.1% full scale). A digital temperature gauge is used to measure the PVT cell temperatures with an accuracy is ±1 K. In zone 2, an in-line viscometer (Hydramotion XL7) is installed inside the oven to measure the viscosity of fluid in the range from 0.1 to 10 000 mPa·s. The viscosity accuracy is ±1% of the reading, and repeatability is ±0.3% of the reading. LED screen displaying measured data from viscometer is connected outside the oven. The pressure of the system is maintained with BPR installed outside of the oven. The BPR pressure is controlled by a gas cylinder, and the effluent is collected by an effluent collector. Moreover, all containers, lines, and valves are cleaned by ethanol and then dried completely for next run.

2.2 | Experimental materials

Fourteen sandpacks of different permeabilities were used in this work to simulate heterogeneous layers environment. The permeabilities of high permeability and low permeability are around 3000×10^{-3} and 500×10^{-3} μm^2, respectively. The sandpack size is 60.0 × 2.5 cm (length × internal diameter). The silica sands including 400 mesh calcium carbonate

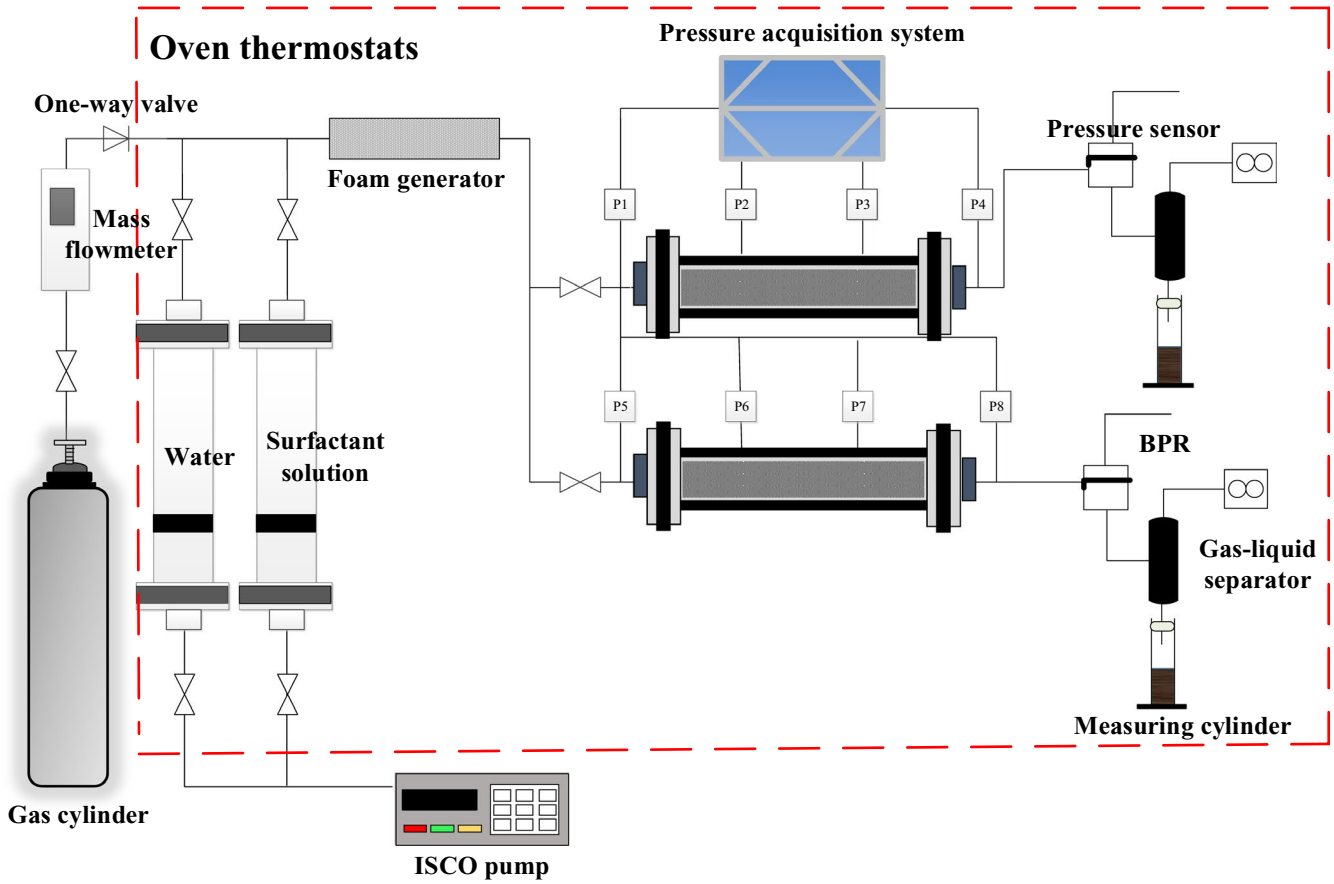

FIGURE 2 Schematic diagram of conventional foam flooding experiment

particles of 8% volume percentage were mixed evenly before packed to the tube. The physical parameters of sandpacks used are presented in Table 1.

Inorganic salt sodium chloride (NaCl), potassium chloride (KCl), and magnesium chloride hexahydrate ($MgCl_2{\cdot}6H_2O$) with the mass concentration of 9057.56, 1627.83, and 1589.49 mg/L were used to prepare the synthetic brine instead of the real brine retrieved from the oilfield because of the complexity and economic cost in offshore platform. All inorganic chemical agents (Purity ≥ 99.5%) were provided by Macklin in Shanghai. The total salinity of synthetic formation brine was 11 492.30 mg/L with the concentration of Na^+, Mg^{2+}, K^+, and Cl^- of 3561.10, 187.92, 852.17, and 6828.11 mg/mL, respectively. The water used was distilled water collected from ultrapure water apparatus (UPD-I-5).

Oil sample and carbon dioxide. The oil sample used in this study was collected from oilfield with viscosity of 5189.8 mPa·s and density of 903.9 kg/m^3 at 25℃. The changing parameters of viscosity and density with temperature are shown in Figure 4, and density has an approximately linear relationship with temperature in Cartesian coordinate system with R-square of 0.994. Carbon dioxide of the purity of 99.9% bought from Tianyuan Inc, was used to prepare the conventional foam.

The reaction formula used in the subsequent experiment is shown in Figure 5. The gas-generating agents and gas-releasing agents are sodium carbonate (Na_2CO_3, with the purity of 99.8%) and hydrochloric acid (HCl, with the purity greater than 99.8%), respectively. The reaction product, sodium chloride, CO_2 foam, and water, have nearly no harm to the environment. Sodium carbonate and hydrochloric acid were purchased from Sinopharm Chemical Reagent Company Limited.

The biological surfactant A2 used was obtained from saponins of camellia oleifera (Figure 6) by a series of esterification reaction and transesterification in different catalysts, which was provided from Qing Tian Zhong Ye Inc. Our previous study has confirmed their good performances on temperature and salt resistance.[35] Acid resistance evaluation test revealed its good acid resistance performance, shown in Figure 7. The mass concentration of A2 used was 0.5%, and the gas-releasing agent was obtained by diluting concentrated hydrochloric acid in a ratio of 1:3.

2.3 | Experimental procedures

2.3.1 | Sandpack flooding experiment

The sandpacks were initially subjected to vacuuming and saturated water treatment, and the core porosity and water permeability were calculated by the weighing method and the Darcy

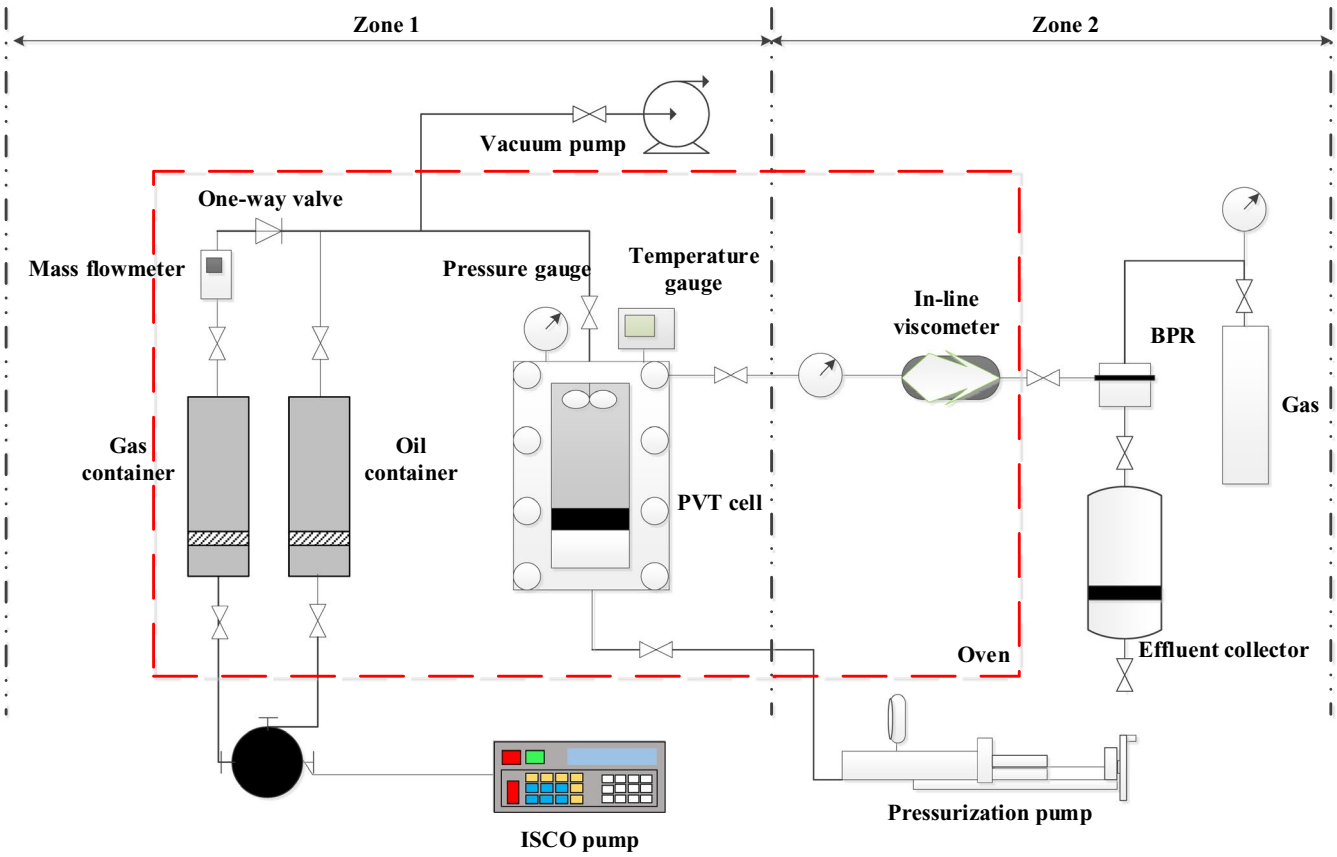

FIGURE 3 Schematic diagram of CO_2 dissolution PVT experiment

TABLE 1 Physical parameters for sandpacks used in this work

Test no.	Length (cm)	Diameter (cm)	Porosity (%)	Permeability ($\times 10^{-3}\mu m^2$)	Permeability ratio
1#	60.0	2.5	41.25	3029	6.13
	60.0	2.5	38.23	494	
2#	60.0	2.5	40.89	2970	6.29
	60.0	2.5	38.14	472	
3#	60.0	2.5	41.13	3013	5.93
	60.0	2.5	38.72	508	
4#	60.0	2.5	41.19	3021	6.10
	60.0	2.5	38.37	495	
5#	60.0	2.5	41.01	3042	6.06
	60.0	2.5	38.35	502	
6#	60.0	2.5	40.78	2982	6.10
	60.0	2.5	38.11	489	
7#	60.0	2.5	41.03	3001	5.97
	60.0	2.5	38.52	503	

formula,[36] respectively. Subsequently, they were preheated in an oven for 3 hours. After that, the experimental oil sample was injected into the sandpack at a constant flow rate of 0.1 mL/min to conduct oil saturation treatment. Flooding experiment started with water flooding of 1.5 PV was conducted at the rate of 1 mL/min. Then, different chemical agents were injected to improve the oil production performance, (a) ISCF systems of 0.25, 0.50, 0.75, 1.00, and 1.25 PV were injected at a rate of 1 min/min by slug injection method, (b) conventional foam was injected at a rate of 2 mL/min with an optimum foam quality of 50%,[37] and (c) ISC system of 1.00 PV was injected at a rate of 1 min/min by slug injection method. Finally, 1.25-2.25 PV

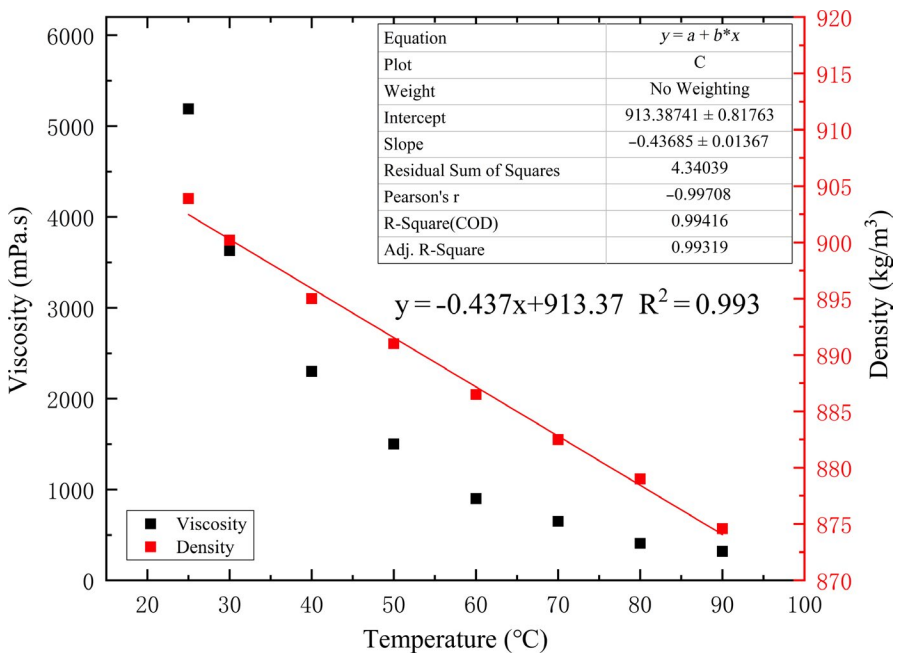

FIGURE 4 Viscosity and density parameters vs temperatures

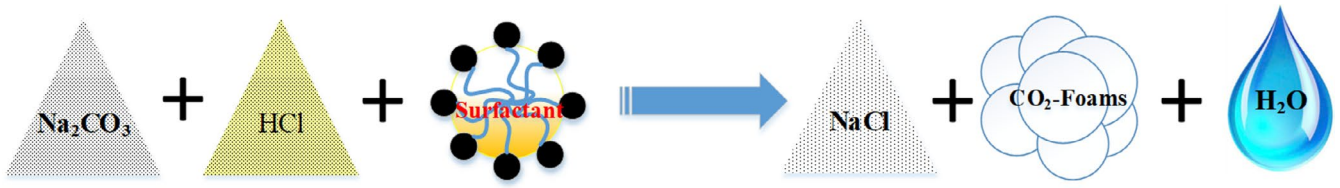

FIGURE 5 Reaction of the formula

subsequent water flooding treatment was carried out at a rate of 1 mL/min. The produced liquids at different stages for the different systems were collected and recorded. In the experiment, the oven control temperature was 60°C (temperature control accuracy ± 0.5°C).

2.3.2 | PVT test experiment

Firstly, the PVT cell was vacuumed for 5 hours before measurement. The gas was injected into the PVT cell with a precise volume control by ISCO and gas flowmeter. Because of the relatively high viscosity of oil sample, it was heated for half hours at 313.15 K before injecting into the PVT cell. After the injection of gas and oil, the oven was set to target temperature (313.15, 333.15, and 353.15 K), and the magnetic mixer equipped inside the PVT cell was operated to enhance the efficiency of mixing of components. The PVT cell pressure was set high sufficiently to exceed to bubble point pressure at the interested temperature in order to have the mixture as a single liquid phase. The system was left for at least 6 hours while using the magnetic mixer. An equilibrium state of the mixture was confirmed by constant temperature, pressure and volume

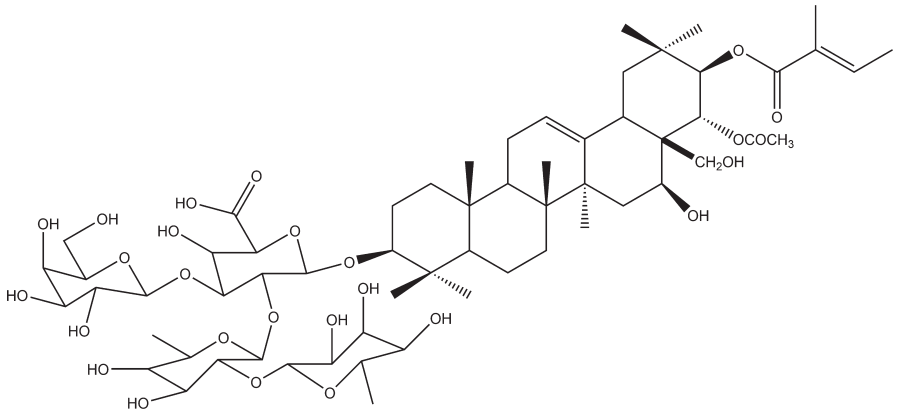

FIGURE 6 biological surfactant: saponins of camellia oleifera

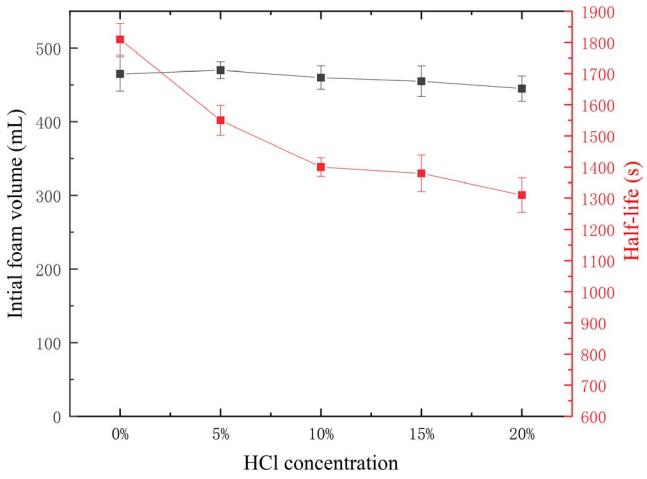

FIGURE 7 Acid resistance performance of surfactant A2

in the PVT cell. Then, the viscosity of oil sample after CO_2 sufficient dissolution at different temperature and pressure was measured by in-line viscometer.

3 | RESULTS AND DISCUSSION

3.1 | Feasibility analysis of ISCF system on enhanced oil recovery

Figure 8 shows the total oil recovery against injected volume curves for 0.25, 0.50, 0.75, 1.00, and 1.25 PV (Test no 1#, 2#, 3#, 4#, and 5# in Table 1). The total oil recovery was initially zero before the injection of water. During initial water flooding, the oil recovery increased rapidly at the beginning. As more water was injected, more oil was produced from the sandpacks; hence, there was a steady increase in total oil recovery as observed in Figure 8. As oil was continuously produced from the sandpacks, the water cut increased, and when it reached about 98%, injection of foaming agents was commenced.

The foaming agents were injected using 2, 4, 6, 8, and 10 slugs for 0.25, 0.50, 0.75, 1.00, and 1.25 PV, respectively. When the first slug was injected, the total oil recovery for both sandpacks remained constant. This is because the first slug injected was sodium carbonate; hence, there was no reaction leading to foam generation in the sandpack. Upon injection of hydrochloric acid as the second slug, the generated energy (pressure) in the sandpacks started to increase rapidly leading to an increase in the total oil recovery. This showed that the reaction between sodium carbonate and hydrochloric acid successfully generated foam in the sandpacks. With further injection of the foaming agents, the total oil recovery continued to increase due to the foam increase forcing more oil to be recovered.

Injection of 0.25 and 0.5 PV of the foaming agents generated small amount of foam which could not effectively block the high permeability sandpack resulting in low total oil recovery values compared with the injection volume of 0.75, 1 and 1.25 PV. Therefore, it should be noted that the more the quantity of the foaming agents injected, the more effective the reaction and the higher the oil recovery. After the injection of the last slug of foaming agents, subsequent water flooding was performed to recover the remaining oil.

During subsequent water flooding stage, water was injected into the sandpacks to produce the remaining oil. At this stage, the foam created could control the mobility of the water injected allowing more oil to be recovered from the sandpacks. The CO_2 gas generated dissolved in the oil reducing the viscosity of the oil, hence allowing more oil to be recovered. The total oil recovery increased slightly during this stage depending on the quantity of the foaming agent injected. It is observed that the total oil recovery for 0.25 PV in the subsequent water flooding stage is

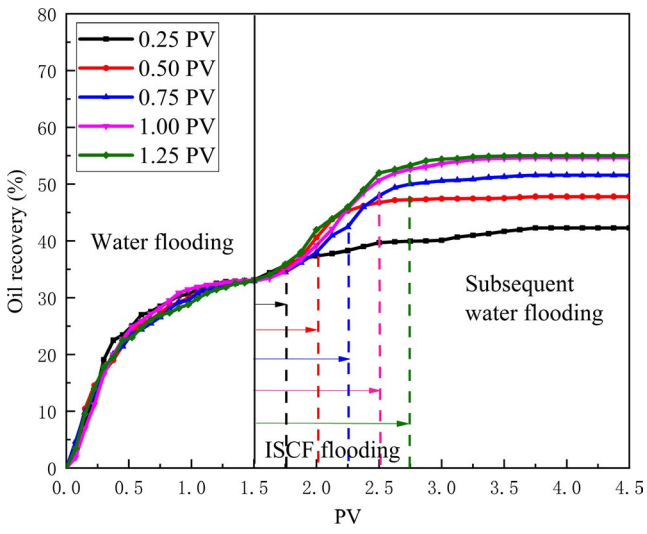

FIGURE 8 Total oil recovery against injected volume curves for 0.25, 0.50, 0.75, 1.00, and 1.25 PV

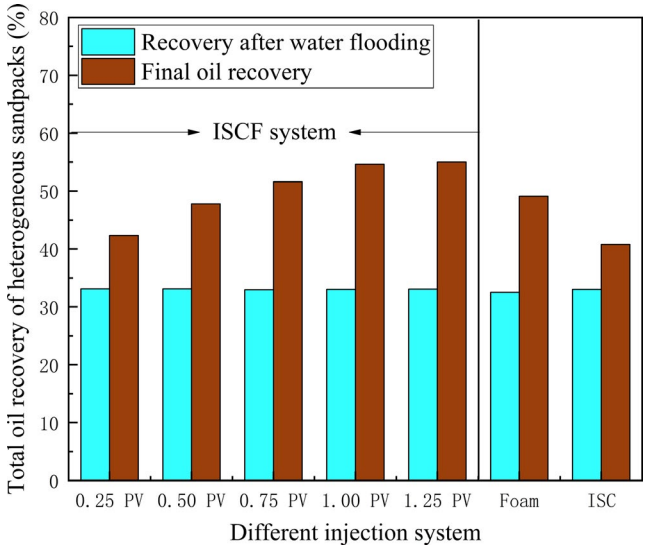

FIGURE 9 Bar chart used for total oil recovery for different injection systems

TABLE 2 Oil displacement efficiency performance for different injection systems

Experiment no	Foaming agents	Injection volume/PV	Water flooding recovery/%	Enhanced oil recovery/%	Final oil recovery/%
#1	ISCF	0.25	33.3	9.0	42.3
#2	ISCF	0.50	33.1	14.7	47.8
#3	ISCF	0.75	32.7	18.9	51.6
#4	ISCF	1.00	33.0	21.6	54.6
#5	ISCF	1.25	33.1	21.9	55.0
#6	Foam	1.00	32.9	16.6	49.5
#7	ISC	1.00	33.0	10.8	43.8

Note: Enhanced oil recovery by foaming agents and subsequent water flooding.

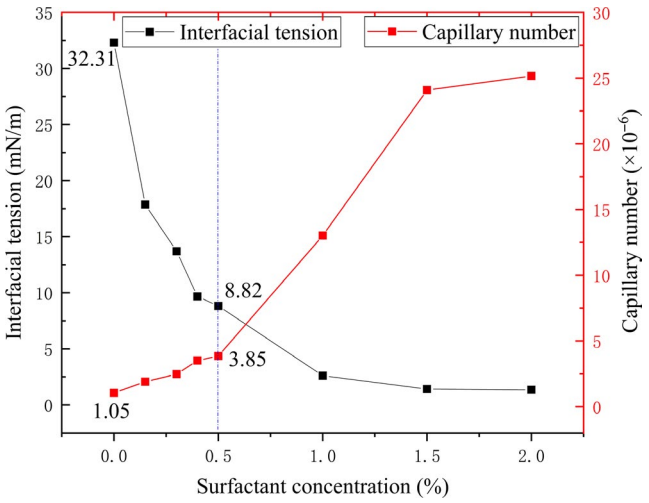

FIGURE 10 Interfacial tensions for generated CO_2 foam (surfactant solutions) and crude oil at 60°C

bigger than that for 1.25 PV since large quantity of remaining oil results in more effective recovery in this stage.

Figure 9 and Table 2 show the bar chart used for total oil recovery and oil displacement efficiency performance for different injection systems, respectively. It can be seen the water flooding recoveries for different systems were all around 33.0%, which depended on the similar physical properties of sandpacks. The oil production performance was improved after injection foaming agents, and the final oil recovery of the parallel sandpacks increased with the increase in injection volume of ISCF system. The final oil recovery of ISCF system at 0.25, 0.50, 0.75, 1.00, and 1.25 PV injection volumes were 42.3%, 47.8%, 51.6%, 54.6%, and 55.0%, respectively, where the enhanced oil recovery by foaming agents was 9.0%, 14.7%, 18.9%, 21.6%, and 21.9%, respectively.

The results indicated that the final recovery of ISCF system almost got to the maximum performance at the ISCF injection volume of 1.0 PV. Continuing to increase the injection volume will not significantly improve the recovery effect. This is because the mechanism of enhanced recovery of the ISCF system mainly depended on the foam generated by the internal reaction. The foam could temporarily block the high permeability sandpack by foam destruction and foam regeneration, and then contributed to the exploitation of crude oil in low permeability sandpack. After the system was injected for a period of time, it would reach a stable state in which the foam was destroyed and regenerated. At this time, the pressure would not increase continuously as the injection amount of the system increased, and the block effect tended to be stable. Besides, compared with the final oil recovery in parallel sandpacks in conventional foam of 49.5%, and in ISC system of 43.8%, the incremental oil recovery by ISCF was much greater than that of conventional foam or ISC system. ISCF could increase oil recovery by 21.6% from heterogeneous multilayer formations of permeability ratio over 6.

3.2 | Mechanism analysis of ISCF system on enhanced oil recovery

3.2.1 | Reduction of interfacial tension

Teclis Tracker H, a drop shape tensiometer with full scale of 20 MPa and 200℃, was used to measure the interfacial tension of oil sample at 60℃. The calculation of interfacial tension was based on Laplace equation.[38-42] More details surface properties measurement was presented in paper.[43] Figure 10 presents the interfacial tensions of generated CO_2 foam and crude oil at 60℃. The results showed that the interfacial tension decreased with the rising surfactant concentration, and it decreased from 32.31 to 8.82 mN/m when the surfactant concentration reaches 0.5%.

Capillary number or critical displacement ratio is a dimensionless number indicating the ratio of the viscous force to the capillary force experienced by the displaced phase. It reflects the balance between different forces in the two-phase displacement process of porous media, which is an important concept of tertiary oil recovery. It can be expressed by:

$$N_e = v\mu/\sigma \quad (1)$$

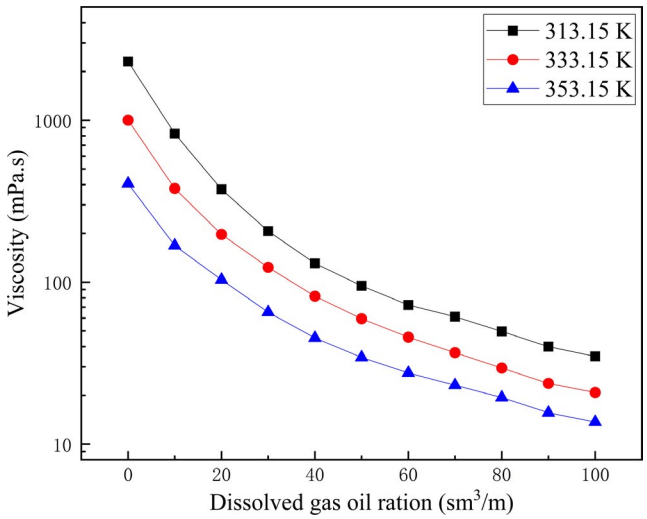

FIGURE 11 Relationship between CO_2 dissolved GOR and viscosity

where N_e is capillary number, v is displacement velocity, μ is the viscosity, and σ is the interface tension between the displacement phase and the displaced phase. It can be seen from the above formula that the way to increase the capillary number is to increase the displacement speed, increase the viscosity of the displacement phase (such as water), and weaken the interfacial tension between the displacement and the displaced phase. So when the interfacial tension decreased from 32.31 to 1.35 mN/m at the surfactant concentration of 2.0%, the capillary number increased about 24 times, which contributed to the tertiary oil recovery.

3.2.2 | Reduction in crude oil viscosity

Figure 11 shows the viscosity of oil sample changing with CO_2 dissolved gas-oil ratio (GOR) at different temperatures. It can be seen that the viscosity decreased rapidly with the increased CO_2 dissolved GOR, and the degree of reduction in the viscosity of crude oil was more pronounced at a low dissolved GOR. The viscosity of crude oil saturated with CO_2 decreased with increasing temperature. CO_2 had significant effects in reducing the viscosity of crude oils, and the maximum viscosity reduction rate in the test range was 98.49%. This is because the intermolecular forces of the crude oil after CO_2 dissolution have changed from the original system, changing from the original liquid-liquid intermolecular force to the liquid-gas intermolecular force. The macromolecular layered structures of resin and asphaltene are destroyed after dissolving CO_2, which resulting in the great reduction in intermolecular forces and intermolecular frictional resistance. Therefore, the degree of viscosity reduction was extremely significant.

In order to analyze the effect of dissolved gas-oil ratio on viscosity reduction effect, the relationship between dissolved gas-oil ratio and viscosity reduction rate at different temperatures was plotted, as shown in Figure 12. The viscosity reduction rate can be expressed as follows:

$$\eta=(\mu_i-\mu_m)/\mu_i\times 100\% \quad (2)$$

where μ_i is the initial viscosity of oil sample at no dissolved CO_2, mPa•s, and μ_m is the viscosity of oil sample at measured dissolved GOR, mPa•s. The results show that the viscosity reduction rate increased with the increase in dissolved gas-oil ratio at each temperature. The reason for the analysis is that the more dissolved carbon dioxide, the smaller the corresponding intermolecular force and intermolecular friction, as well as the better the viscosity reduction effect. Moreover, as the dissolved gas-oil ratio increased, the rate of decrease in viscosity reduction was different. When the dissolved GOR was <50 sm^3/m^3, the viscosity reduction effect increased rapidly with the dissolved GOR, and the viscosity reduction rate reached over 90% at the dissolved GOR of 50 sm^3/m^3, which indicating that the viscosity reduction performance was good even at low in situ CO_2 dissolution condition.

3.2.3 | "Intelligent" acidification

In order to study the "intelligent" acidification in parallel sandpack flooding process, the produced liquid samples were

TABLE 3 Ca^{2+} concentration of produced liquid after flooding

Test no.	System	Collection time	Ca^{2+} concentration for high permeability (mg/L)	Ca^{2+} concentration for low permeability (mg/L)
4#	ISCF	I: After injecting 0.5 PV	29.4	22.7
		II: After injecting 0.75 PV	36.1	31.3
		III: After injecting 1.0 PV	39.7	32.9
6#	Foam	I: After injecting 0.5 PV	< 0.1	< 0.1
		III: After injecting 1.0 PV	< 0.1	< 0.1
7#	ISC	I: After injecting 0.5 PV	39.1	8.6
		II: After injecting 0.75 PV	45.2	10.1
		III: After injecting 1.0 PV	44.6	9.7

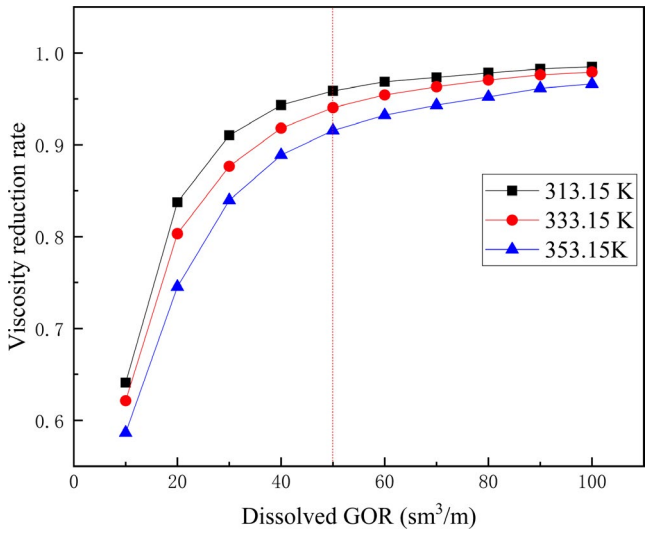

FIGURE 12 Relationship between CO_2 dissolved GOR and viscosity reduction rate

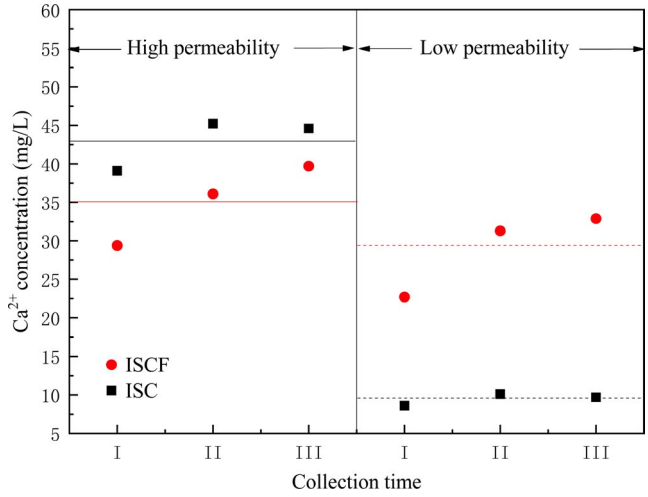

FIGURE 13 Ca^{2+} concentration of produced liquid at different collection time for ISCF and ISC systems

collected and analyzed. Sixteen produced liquids were collected from three groups of flooding experiments (4#, 6#, and 7# in Table 1) based on different flooding conditions, and the Ca^{2+} concentration for each sample was measured by ICP-MS in WeiPu Analysis Testing Center, Shanghai. The parameters were measured for three times, and average values are presented in Table 3. The results displayed Ca^{2+} concentrations of four samples collected from conventional foam experiment were <0.1 mg/L, which was because weak carbonic acid formed by CO_2 in water could not cause effective reaction with $CaCO_3$.

Figure 13 shows the Ca^{2+} concentration of produced liquid at different collection time for ISCF and ISC systems. The average Ca^{2+} concentration of produced liquid collected from high permeability sandpacks of 43.0 mg/L (black solid line in Figure 13) in ISC system was much higher than that in low permeability sandpack of 9.5 mg/L (black dash line in Figure 13), because lower flow resistance existed in high permeability sandpack for injection liquids. Whereas in ISCF system, the average Ca^{2+} concentration of produced liquid collected from high permeability sandpacks of 35.1 mg/L (red solid line in Figure 13) was just little higher than that in low permeability sandpack of 29.0 mg/L (red dash line in Figure 13). Because the plugging caused by viscosity of foam made more agents flow into low permeability sandpacks, which was one expression of "intelligent" acidizing, namely evenly distribute the acid solution in heterogeneous formations. Moreover, the big difference of flow amount of agents in high permeability sandpacks between ISCF and ISC systems did not cause a huge difference in Ca^{2+} concentration of produced liquid. This is because that the high apparent viscosity in situ foam can increase the swept volume which contributed to the even distribution of limited acid in homogeneous formation, which also presented the "intelligent" acidification.

4 | CONCLUSIONS

In situ CO_2 foam was firstly proposed by combining sodium carbonate anhydrous, hydrochloric acid, and bio-based surfactant. The performance for ISCF system EOR was investigated systematically in heterogeneous sandpacks at 60℃. The primary conclusions in this work were as follow:

1. ISCF could increase oil recovery from heterogeneous multilayer formation of permeability ratio over 6, and displacement efficiency increased with the injection volume increased before injection of 1 PV. The incremental oil recovery by ISCF was much greater than that of conventional foam or in situ CO_2 (ISC) without foam under the same injection conditions.
2. The generated CO_2 foam could reduce the interfacial tension between displacement phase and displaced phase effectively which contributed to the great reduction of capillary number.
3. The CO_2 dissolution could greatly reduce the viscosity of crude oil, and the highest viscosity reduction rate at 60°C could be as high as 98%.
4. The Ca^{2+} concentration of produced liquids analysis presented the "intelligent" acidification of ISCF, and the spontaneously generated CO_2 foam contributed to the "intelligent" distribution of acid solution in heterogeneous sandpacks.

ACKNOWLEDGMENTS

This work was financially supported by the National Natural Science Foundation of China (Grant 51604292), the Natural Science Foundation of Shandong Province, China (Grant

ZR2016EEB29), the National Science and Technology Major Project of China (Grant 2016ZX05012-002-004), the Fundamental Research Funds for the Central Universities (Grant R1602013A), the Fundamental Research Funds for the Central Universities (Grant 17CX02014A), and the Innovation Project Funds for the Central Universities (Grant YCX2017024). We sincerely thank other members in the Foam Fluid Research Center in China University of Petroleum (East China) for helping with the experimental research.

ORCID

Hailong Chen https://orcid.org/0000-0002-6715-0383

REFERENCES

1. Srivastava RK, Huang SS, Dong MZ. Asphaltene deposition during CO_2 flooding. *SPE Prod Facil*. 1999;14(04):235-245.
2. Ghedan S. Global laboratory experience of CO_2-EOR flooding. SPE/EAGE reservoir characterization and simulation conference. 2009, SPE-125581.
3. Lake LW. *Enhanced oil recovery*. Englewood Cliffs, NJ: Prentice Hall; 1989.
4. Lake LW, Schmidt RL, Venuto PB. A niche for enhanced oil recovery in the 1990s. *Oil Gas J*. 1990s;88(17):62-67.
5. Rossen WR. Foams in enhanced oil recovery. *Surfactant Sci Ser*. 1996;57:413-464.
6. Koval EJ. A method for predicting the performance of unstable miscible displacement in heterogeneous media. *Old SPE J*. 1963;3(2):145-154.
7. Li RF, Yan W, Liu S, Hirasaki G, Miller C. Foam mobility control for surfactant enhanced oil recovery. *SPE J*. 2010;15(4):928-942.
8. Talebian SH, Masoudi R, Tan IM, Zitha PLJ. Foam assisted CO_2-EOR; concepts, challenges and applications. SPE enhanced oil recovery conference, 2-4 July, Kuala Lumpur, Malaysia, 2013; SPE-165280-MS.
9. Kovscek AR, Tadeusz WP, Radke CJ. Mechanistic foam flow simulation in heterogeneous and multidimensional porous media. *SPE J*. 1997;2(4):511-526.
10. Rossen WR, Van Duijn CJ, Nguyen QP, Shen C, Vikingstad AK. Injection strategies to overcome gravity segregation in simultaneous gas and water injection into homogeneous reservoirs. *SPE J*. 2010;15(1):76-90.
11. Hirasaki GJ, Lawson JB. Mechanisms of foam flow in porous media: apparent viscosity in smooth capillaries. *Old SPE J*. 1985;25(2):176-190.
12. Hosseininasab SM, Zitha PLJ. Investigation of chemical-foam design as a novel approach toward immiscible foam flooding for enhanced oil recovery. *Energy Fuels*. 2017;31(10):10525-10534.
13. Sun Q, Li ZM, Li SY, Jiang L, Wang JQ, Wang P. Utilization of surfactant-stabilized foam for enhanced oil recovery by adding nanoparticles. *Energy Fuels*. 2014;28(4):2384-2394.
14. Bernard GG, Jacobs WL. Effect of foam on trapped gas saturation and on permeability of porous media to water. *Soc Petrol Eng J*. 1965;5(4):295-300.
15. Nguyen QP. Systematic study of foam for improving sweep efficiency in chemical enhanced oil recovery. *Surgery*. 2011;142(1):20-25.
16. Zhu JY, Yang ZZ, Li XG, Song ZC, Liu ZW, Xie SY. Settling behavior of the proppants in viscoelastic foams on the bubble scale. *J Petrol Sci Eng*. 2019;181:106216.
17. Zhu JY, Yang ZZ, Li XG, Hou LL, Xie SY. Experimental study on the microscopic characteristics of foams stabilized by viscoelastic surfactant and nanoparticles. *Colloids and Surface A*. 2019;572:88-96.
18. Farajzadeh R, Wassing BM, Boerrigter PM. Foam assisted gas-oil gravity drainage in naturally-fractured reservoirs. *J Petrol Sci Eng*. 2012;94–95(5):112-122.
19. Kennedy DK, Kitziger FW, Hall BE. Case study on the effectiveness of nitrogen foams and water zone diverting agents in multistage matrix acid treatments. *SPE Prod Eng*. 1992;7(2):203-211.
20. Eftekhari AA, Krastev R, Farajzadeh R. Foam stabilized by fly-ash nanoparticles for enhancing oil recovery. *Ind Eng Chem Res*. 2015;54(50):12482-12491.
21. Fei Y, Zhu J, Xu B, Li X, Gonzalez M, Haghighi M. Experimental investigation of nanotechnology on worm-like micelles for high-temperature foam stimulation. *J Ind Eng Chem*. 2017;50:190-198.
22. Zhang C, Li ZM, Li SY, et al. Enhancing sodium bis(2-ethylhexyl) sulfosuccinate injectivity for CO_2 foam formation in low-permeability cores: dissolving in CO_2 with ethanol. *Energy Fuels*. 2018;32(5):5846-5856.
23. Zhang C, Li ZM, Sun Q, Wang P, Wang SH, Liu W. CO_2 foam properties and the stabilizing mechanism of sodium bis (2-ethylhexyl) sulfosuccinate and hydrophobic nanoparticle mixtures. *Soft Matter*. 2015;12(3):946-956.
24. Mohd TAT, Harun A, Ghazali NA, Alias N, Yahya E. Interfacial tension dependence on nanoparticle surface modification for stabilization of CO_2 foam in EOR: an overview. *Adv Mater Res*. 2015;1113(53):637-642.
25. Wang SS, Chen CL, Shiau B, Harwell JH. In-situ CO_2 generation for EOR by using urea as a gas generation agent. *Fuel*. 2018;217:499-507.
26. Wang SS, Kadhum MJ, Chen CL, Shiau B, Harwell JH. Harwell, development of in situ CO_2 generation formulations for enhanced oil recovery. *Energy Fuels*. 2017;31:13475-13486.
27. Wang SS, Kadhum M, Yuan QW, Shiau B, Harwell JH.Carbon dioxide in situ generation for enhanced oil recovery. Carbon management technology conference, 17–20 July, Houston, Texas, USA, 2017;CMTC-486365-MS.
28. Wang SS, Chen CL, Li K, Yuan N, Shiau B, Harwell JH. In situ CO_2 enhanced oil recovery: parameters affecting reaction kinetics and recovery performance. *Energy Fuels*. 2019;33:3844-3854.
29. Wang SS, Li K, Chen CL, Onyekachi O, Shiau B, Harwell JH. Isolated mechanism study on in situ CO_2 EOR. *Fuel*. 2019;254:115575.
30. Zhu DY, Hou JR, Wang JF, Wu X, Wang P, Bai BJ. Acid-alternating-base (AAB) technology for blockage removal and enhanced oil recovery in sandstone reservoirs. *Fuel*. 2018;215:619-630.
31. Wang Y, Hou J, Tang Y. In-situ CO_2 generation huff-n-puff for enhanced oil recovery: laboratory experiments and numerical simulations. *J Petrol Sci Eng*. 2016;145:183-193.
32. Abdelgawad K, Mahmoud M. In situ generation of CO_2 to eliminate the problem of gravity override in EOR of carbonate reservoirs. SPE middle east oil & gas show and conference, Society of Petroleum Engineers, 2015.
33. Jin FY, Wei P, Pu WF, Zhang L, Qian Z, Wu GS. Experimental study of in-situ CO_2 foam technique and application in Yangsanmu Oilfield. *J Surfact Deterg*. 2016;19:1231-1240.

34. Jin FY, Wei P, Pu WF, Zhang L, Qian Z, Wu GS. Investigation on foam self-generation using in situ carbon dioxide (CO_2) for enhancing oil recovery. *J Surfact Deterg*. 2018;21:399-408.
35. Wang F, Chen HL, Alzobaidi S, Li ZM. Application and mechanisms of self-generated heat foam for enhanced oil recovery. *Energy Fuels*. 2018;32:9093-9105.
36. Dai C, Wang K, Liu YF, Li H, Wei ZY, Zhao MW. Reutilization of fracturing flowback fluids in surfactant flooding for enhanced oil recovery. *Energy Fuels*. 2015;29(4):2304-2311.
37. Li SY, Li ZM, Li BF. Experimental study and application on conformance control using high-temperature foam. *J Petrol Sci Eng*. 2011;78(3):567-574.
38. Li HZ, Yang DY, Tontiwachwuthiku P. Experimental and theoretical determination of equilibrium interfacial tension for the solvent(s)-CO_2-heavy oil systems. *Energy Fuels*. 2012;26:1776-1786.
39. Yang DY, Gu YA.Visualization of interfacial interactions of crude oil-CO_2 systems under reservoir. In: SPE/DOE symposium on improved oil recovery, 17–21 April, Tulsa, Oklahoma, 2004; SPE 89366.
40. Yang DY, Tontiwachwuthikul P, Gu YA. Interfacial tensions of the crude oil + reservoir brine + CO_2 systems at pressures up to 31 MPa and temperatures of 27°C and 58°C. *J Chem Eng Data*. 2005;50:1242-1249.
41. Zolghadr A, Escrochi M, Ayatollahi S. Temperature and composition effect on CO_2 miscibility by interfacial tension measurement. *J Chem Eng Data*. 2013;58:1168-1175.
42. Li HZ, Yang DY. Phase behavior of C3H8-n-C4H10-heavy oil systems at high pressures and elevated temperatures. In: SPE heavy oil conference Canada, 12-14 June, 2012;Calgary, Alberta, Canada, SPE 157744.
43. Li SY, Li ZM, Sun XN. Effect of flue gas and n-hexane on heavy oil properties in steam flooding process. *Fuel*. 2017;187:84-93.

How to cite this article: Chen H, Li Z, Wang F, Li A, Wanambwa S, Lu T. Experimental study on the enhanced oil recovery by in situ foam formulation. *Energy Sci Eng*. 2020;8:1092–1103. https://doi.org/10.1002/ese3.570